Journal of Asian Earth Sciences 231 (2022) 105213

Contents lists available at ScienceDirect

Journal of Asian Earth Sciences

journal homepage: www.elsevier.com/locate/jseaes

Strontium isotope stratigraphy of late Cenozoic fossiliferous marine deposits in North Borneo (Brunei, and Sarawak, Malaysia)

László Kocsis [a,b,*], Antonino Briguglio [c], Anna Cipriani [d,e], Gianluca Frijia [f], Torsten Vennemann [a], Claudia Baumgartner [g], Amajida Roslim [b]

[a] Institute of Earth Surface Dynamics, University of Lausanne, Rue de la Mouline, 1015 Lausanne, Switzerland
[b] Geology Group, Faculty of Science, Universiti Brunei Darussalam, Jalan Tungku Link, Gadong BE1410, Brunei Darussalam
[c] DI.S.T.A.V, Dipartimento di Scienze della Terra, dell'Ambiente e della Vita Università degli Studi di Genova, Corso Europa, 26, I – 16132 Genova, Italy
[d] Dipartimento di Scienze Chimiche e Geologiche, Università di Modena e Reggio Emilia, Modena, Italy
[e] Lamont-Doherty Earth Observatory, Columbia University, Palisades, NY, USA
[f] Dipartimento di Fisica e Scienze della Terra University of Ferrara, via Saragat 1, 44121 Ferarra, Italy
[g] Institute of Earth Sciences, University of Lausanne, Rue de la Mouline, 1015 Lausanne Switzerland

ARTICLE INFO

Keywords:
$^{87}Sr/^{86}Sr$
SIS
Neogene
Southeast Asia
Stable isotopes
Trace elements

ABSTRACT

Neogene marine deposits of North Borneo are locally very rich in fossils that provide glimpses into the past biodiversity. However, dating these onshore sediments with biostratigraphy is often hampered by the lack and/or the poor preservation state of index fossils. Therefore, the fossiliferous sites were targeted with strontium isotope stratigraphy (SIS) to obtain higher precision relative dating. Well-preserved macrofossils were screened using a multidisciplinary approach, and $^{87}Sr/^{86}Sr$ ratios of the most pristine remains were used to date the embedding sediments. Most of the measured ages fall in the expected chronostratigraphic framework established by large scale studies for the region. The oldest, Burdigalian (early Miocene) ages were measured for the Sibuti Formation in Sarawak (17.71 ± 0.2My and 16.7 ± 0.2My) followed by a Serravallian (middle Miocene) age within the Belait Fm in Brunei (12.1 + 1.4/-1.2My). Eight localities from the younger units, the Miri and Seria formations in Brunei, gave a range in age from 10.5 ± 1 to 7.0 + 0.9/-0.5My (Tortonian-Messinian). Reworked fossil assemblages from Tutong beach were also investigated and the SIS ages of Late Miocene support an origin from the younger part of the Seria Fm. One locality, in Lumapas where limestone crops out in Brunei, gave an unexpected younger age (Tortonian, late Miocene, 10.6 ± 1My) compared to estimates projected for its assumed stratigraphic position in the lower Belait Formation (late Burdigalian). These challenging data require more research, yet if the young age is accepted, the stratigraphic situation of the limestone needs further revision.

1. Introduction

Borneo is the world's third largest island situated in the center of the Indo-Australian Archipelago (IAA), a region with the highest biodiversity today (Hoeksema, 2007; Bellwood et al., 2012 and references therein) that evolved since the Miocene (Renema et al., 2008). However, paleontological research in Borneo and related paleobiodiversity synthesis are sparse, mainly due to the lack of available outcrops related to dense vegetation of the tropical rainforest, lack of systematic and focused sampling, and lack of research on potential fossiliferous sedimentary successions. Previous geological investigations in Borneo concentrated on mapping for road constructions and for industrial resources (ores, oil and gas, etc.) (e.g., Liechti et al., 1960; Wilford, 1961), and though fossil content of sedimentary rocks were recorded, detailed paleontological descriptions (e.g., taxonomy, ecology) were rare (Beets, 1947, 1983; Nuttall, 1961, 1965; Stinton, 1962). Over the last 10–20 years, however, more information was collected, especially from marine deposits of East Kalimantan (e.g., Novak and Renema, 2015; Di Martino et al., 2015; Kusworo et al., 2015) and North Borneo (e.g., Collins et al., 2003; Mihaljević et al., 2014; Simon et al., 2014; Harzhauser et al., 2018; Kocsis et al., 2019, 2020, 2021; Roslim et al., 2019, 2020, 2021).

In order to constrain detailed, time-related changes in paleobiodiversity, the age of the fossiliferous deposits must be well assessed.

* Corresponding author.
E-mail address: laszlo.kocsis@unil.ch (L. Kocsis).

https://doi.org/10.1016/j.jseaes.2022.105213
Received 26 October 2021; Received in revised form 29 March 2022; Accepted 3 April 2022
Available online 12 April 2022

The stratigraphic framework of North Borneo has been recently updated using sequence stratigraphy, biostratigraphy, and tectonic analysis (Hennig-Breitfeld et al., 2019; Lunt, 2019; Lunt and Madon, 2017, Morley et al., 2021). The data of these studies are mainly derived from offshore exploration of oil companies (boreholes and seismic profiles). In contrast to small onshore outcrops precise correlations are often difficult. Moreover, important index microfossils, such as calcareous nannoplankton and planktonic foraminifera are either absent due to shallow siliciclastic depositional conditions, or badly preserved due to their low preservation potential under tropical weathering. However, when well-preserved marine carbonate macrofossils are available, they can be analyzed for strontium isotope ratios ($^{87}Sr/^{86}Sr$), and the data can be compared with the marine Sr-evolution curve to estimates numerical ages (i.e., Strontium Isotope Stratigraphy – SIS, see McArthur et al., 2001; 2020). Such an approach has been applied to carbonate rocks drilled in the South China Sea off the coast of North Borneo (Vahrenkamp, 1998; Grötsch and Mercadier, 1999; Lunt and Madon 2017), to Bornean onshore carbonates (Lunt, 2014) and well-preserved calcareous fossils (Renema et al., 2015; Kocsis et al., 2018, 2021).

This study presents SIS ages from fossil-rich outcrops from northern Sarawak (Miri region, Malaysia) and Brunei Darussalam with the aim to provide better age estimates. This then helps to compare contemporaneous paleofaunas in Southeast Asia and evaluate changes in biodiversity through time within the region. The obtained strontium isotope ages are compared and correlated to the cycles of the most recent sequence biostratigraphic framework of the region presented by Morley et al. (2021).

1.1. Strontium isotope stratigraphy (SIS)

Aquatic organisms generally record the chemical and isotopic compositions of the ambient water, and with appropriate chemical and isotopic fractionations such compositions are also reflected in their mineralized parts (e.g., shells, tests, teeth). However, biological (i.e., vital effect) as well as diagenetic processes may override equilibrium compositions, which need to be considered for paleoenvironmental and paleoclimatic reconstructions. One way to overcome such issues is to use the same taxon or similar taxa, hence relative variations within the same taxa could be taken to reflect environmental changes. However, even if there may be small vital effect in terms of Sr incorporation in the biominerals, there is apparently no measurable fractionation during biomineralization for the Sr-isotope ratio ($^{87}Sr/^{86}Sr$) (e.g., Hodell et al., 1991; Veizer et al., 1997; McArthur et al., 2001). The residence time of Sr in seawater ($>10^6$ years) is longer than the mixing time of the oceans ($\sim10^3$ years), which eventuates a unique $^{87}Sr/^{86}Sr$ ratio for the ocean (Burke et al., 1982; DePaolo and Ingram, 1985; Veizer, 1989; Frank, 2002) that can be recorded in biominerals of marine organisms. The $^{87}Sr/^{86}Sr$ of the dissolved Sr in seawater, however, varied through geological time related to proportionally different input of Sr in the oceans (i.e., crustal vs. mantle end-members). This time dependent variation in $^{87}Sr/^{86}Sr$ in the open ocean is the basis for Strontium Isotope Stratigraphy (SIS) that enables dating marine sedimentary units (e.g., Koepnick et al., 1985; Hodell et al., 1991; Veizer et al., 1997; McArthur et al., 2001, 2020).

In order to date marine rocks, pristine and unaltered remains are necessary. Diagenesis, can affect original open marine Sr-isotopic ratios of the analyzed samples, depending on the degree of post-mortem alteration and recrystallization as well as the composition of the diagenetic fluid. SIS is best applied to open marine deposits, however when it comes to coastal and estuarine shallow water settings the above mentioned issues may well be enhanced. In order to assess the quality of the samples besides macro-and microscopic observations, the original mineralogy (e.g., XRD for aragonite) and cathodoluminescent properties or SEM microstructural analyses are often examined. These are frequently supplemented by minor and trace element (Mg, Sr, Fe, Mn) and/or stable oxygen and carbon isotope analyses (e.g., McArthur et al., 2001, 2020).

2. Geological setting and the studied localities

The geological investigation of North Borneo was initially driven by a search for natural resources via detailed mapping of the region (e.g., Liechti et al., 1960; Wilford, 1961), but paleontological data were occasionally mentioned and discussed as well (e.g., Nuttall, 1961; James, 1984). This study focuses on fossiliferous units in Sarawak and Brunei. The study area is located in the eastern side of the Miri Zone (Haile, 1974), where we concentrated on onshore Neogene deposits (Fig. 1). The sedimentary rocks indicate depositional environments with a general, time related shift from a deeper, open marine setting towards coastal deltaic facies, in some cases with a stronger fluvial influence (Roslim et al., 2020). The lower and middle Miocene is represented by deep marine sediments consisting of clayey rocks (Setap Shale Formation) sometimes with a higher carbonate content (Sibuti Formation), but also by thick reef-related limestone deposits (Niah Mountain i.e., Subis Formation). In the middle Miocene the hinterland uplifted exposing older rocks (Crocker Range) resulting in a higher amount of siliciclastic sediment supplied to adjacent basins via several deltaic systems (Saller and Blake, 2003; Lambiase et al., 2003; Lambiase and Cullen, 2013; Kessler and Jong, 2015). The Middle and Upper Miocene is characterized by tidal- and wave-dominated, rather sandy sediments (Belait and Lambir formations) adjacent to shallow, coastal marine successions (Miri and Seria formations). The latter often consists of several stacked-up small-scale sequences with higher clay content at their base (e.g., Liechti et al., 1960; Wilford, 1961). Some authors consider all these deposits as belonging to one lithostratigraphic unit, the Belait Formation (e.g., Back et al., 2001; Morley et al., 2003). The prograding deltas gradually filled up the basins, and by the Pliocene more fluvial and lagoonal sediments were formed together with occasional thick conglomerate beds and lignite bearing horizons (Liang Formation). Some of the described sediments were deformed and tilted by compressive tectonics during the Mio-Pliocene that resulted in large syncline-anticline structures recorded both onshore and offshore (Morley et al., 2003). The sequence stratigraphic frameworks for these deposits have been proposed by several authors, and on this basis the overall depositional ages of the region's sedimentary cycles were well assessed (e.g., Morrison and Wong, 2003; Saller and Blake, 2003; Torres et al., 2011; Morley et al., 2021). However, the correlation of onshore small-scale outcrops with the established sequences can be challenging due to a lack of biostratigraphic markers and/or their poor preservation state.

Several Neogene outcrops have been investigated for their fossil contents in the past years in Sarawak (Malaysia) and Brunei Darussalam in Northern Borneo (e.g., Wannier et al., 2011; Kocsis et al., 2020, 2021; Roslim et al., 2020, 2021). This study targets the most fossiliferous sections with Strontium Isotope Stratigraphy (SIS), in order to obtain best possible estimates of numerical ages for each site and to correlate them with the cycles of the sequence biostratigraphic framework provided by Morley et al. (2021). SIS combined with biostratigraphy was used, in the recent years, to date one of the most fossiliferous sites in Brunei at the Ambug Hill in the Tutong District (Kocsis et al., 2018), and SIS also helped to trace the origin of reworked fossils found on the Penanjong beach in Brunei (Kocsis et al., 2021). In the present research thirteen new sites are included from three different structural areas (Table 1, Fig. 1):

(1) Two outcrops of the Sibuti Formation in Sarawak Malaysia described in Wannier et al. (2011), where marlstone deposits yield rich mollusk, crustacean, and coral fauna.

(2) Seven localities from the Belait syncline (western flank of the Jerudong anticline) in Brunei, from which six sites expose shallow marine siliciclastic sediments of the Miri and Seria formations (e.g., Collins et al., 2017; Roslim et al., 2020). Based on bedding structure and the dip-direction of the beds, the relative ages of the outcrops get younger

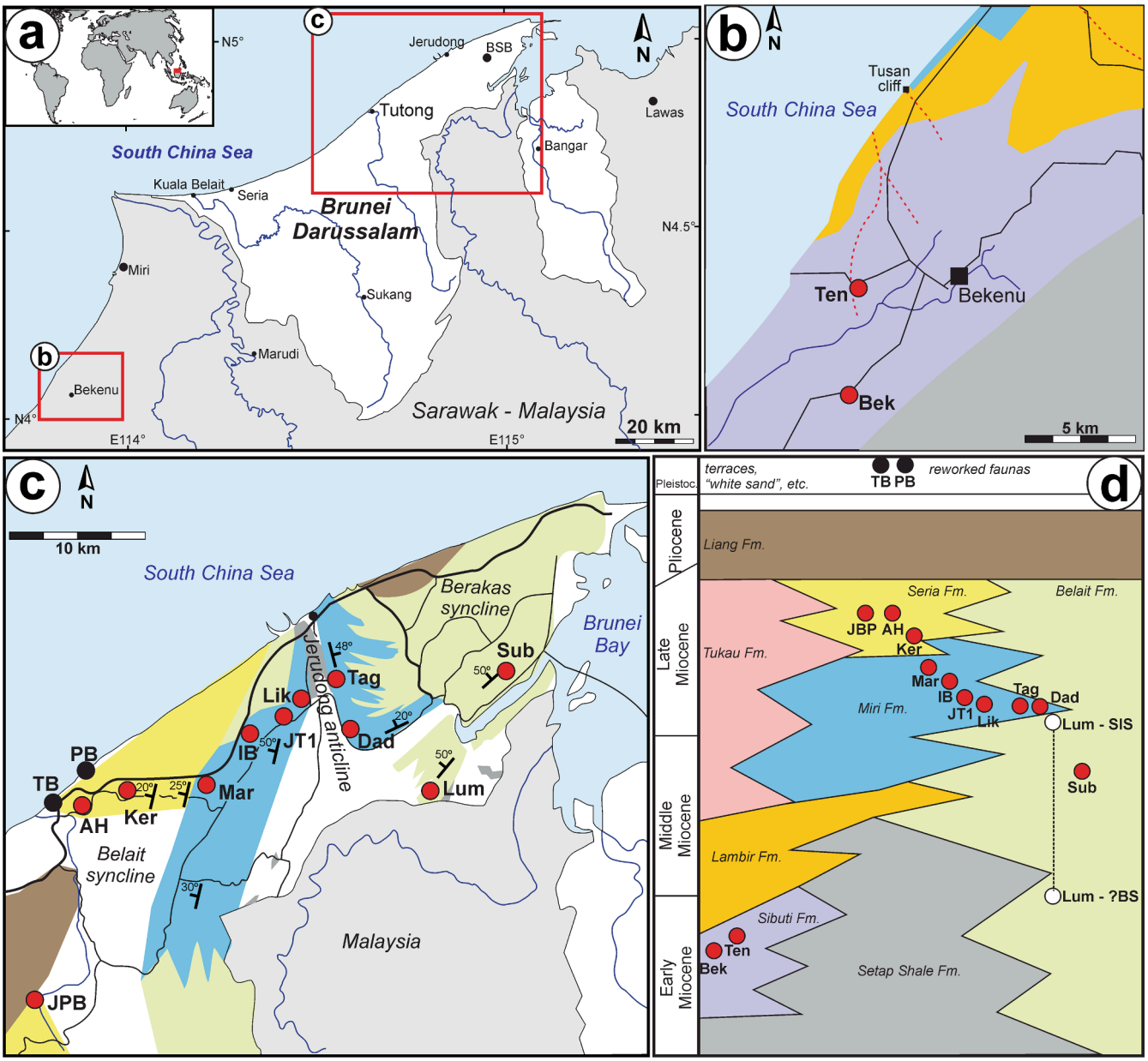

Fig. 1. Geographic position of the studied localities and their time related distribution within the corresponding lithostratigraphic units. The color code in the maps (b-c) corresponds to rock units indicated in Fig. 1d. Abbreviations of the outcrops (see also Table 1): Bek – Bekenu road; Ten – Tengah; Lum – Lumapas limestone; Sub – Subok; Dad – Dadap; Tag – Tagap; LK – Lion King; JT1 – Tanjong Nangka site; IB – Ikas Bandung; Mar – Maraburong; Ker- Keriam village; JPB – Jalan Pak Bidang; TB – Tutong beach reworked fauna. In addition, two previously studied localities with Sr-isotope are shown: AH – Ambug Hill (Kocsis et al., 2018); PB – Penanjong beach reworked assemblage (Kocsis et al., 2021). Note that the older position of the Lumapas limestone (Lum) is based on preliminary biostratigraphic data (BS) (Briguglio et al., 2017), however this is challenged here by the SIS data showing the alternativ younger age in Fig. 1d.

towards the NW. The seventh site is the Tutong beach from where remains of reworked marine vertebrates were recently discovered and hence included in this study.

(3) Four sites from the Berakas syncline in Brunei. Two are clay-rich deposits of the Miri Formation at the eastern flank of the Jerudong anticline (Fig. 1). One locality belongs to the Belait Formation (Lambiase and Cullen, 2013), which crops out towards the South and East with dominantly sandy facies poor in body fossils. Nevertheless, a fossil-rich claystone with oyster mounds was discovered within this formation at Subok (Kocsis et al., 2020; Roslim, 2021). This latter was sampled for SIS. The fourth site is from Lumapas where Brunei's only limestone occurrence can be found. These calcareous beds were reported to be intercalated within the older series of the Belait Formation (Wilford, 1961).

3. Materials and methods

From the studied outcrops well-preserved macrofossils were collected and prepared for geochemical analyses. Mollusks that commonly occur and originally have calcite shells such as Pectenidae (scallops) and Osteridae (oysters) were first targeted. The former ones were preferred as they are stenohaline marine organisms, in contrast to certain oyster species that can also inhabit brackish environments. Moreover, the coarsely layered shells of the oysters can entrap sediment particles, as they frequently grow in more wave-agitated environments. If these two taxa were absent, other bivalves, sea urchin spines, or originally aragonite biominerals such as fish otolith or gastropod operculum, or in some cases vertebrate remains (teeth and bones, i.e., bioapatite) were included (Table 2).

Table 1
List of the studied sites with age ranges reported in literature.

		Latitude (N°)	Longitude (E°)	Lithostratigraphy	Lithology	Age range	**Geological References**
Sarawak, Malaysia							
Bekenu-Niah Road	Bek	*4.016369*	*113.803871*	Sibuti Fm.	marlstone	Early-Midddle Miocene	Wannier et al., 2011
Kh. Tengah	Ten	*4.056760*	*113.809338*	Sibuti Fm.	marlstone with coral banks	Early-Midddle Miocene	Wannier et al., 2011
Belait syncline							
Lion King outcrop	LK	*4.893287*	*114.833090*	Miri Fm.	claystone	Late Miocene	Back et al., 2005
Tanjong Nangka	JT1	*4.872805*	*114.820647*	Miri Fm.	claystone	Late Miocene	Back et al., 2005; Collins et al., 2017
Ikas Bandung	IB	*4.866543*	*114.795070*	Miri Fm.	claystone	Late Miocene	Roslim et al., 2020
Maraburong	Mar	*4.824283*	*114.758736*	Miri Fm.	claystone	Late Miocene	Roslim et al., 2020
Keriam	Ker	*4.816958*	*114.702387*	Seria Fm.	claystone	Late Miocene	Roslim et al., 2020
Ambug Hill*	AH	*4.808439*	*114.673204*	Seria Fm.	claystone	Late Miocene	Kocsis et al., 2018
Penanjong Beach*	PB	*4.840554*	*114.676480*	reworked		Late Miocene	Kocsis et al., 2021
Tutong beach	TB	*4.807001*	*114.659907*	reworked			
Jalan Pak Bidang	JPB	*4.674966*	*114.637201*	Seria Fm.	claystone	Late Miocene	Roslim et al., 2020
Berakas syncline							
Lumapas reef	Lum	*4.817994*	*114.922256*	?Belait Fm.	limestone	? Early Miocene	Wilford, 1961
Jalan Subok	Sub	*4.911256*	*114.988254*	Belait Fm.	oyster banks in claystone	Middle Miocene	Lambiase and Cullen, 2013
Dadap	Dad	*4.870174*	*114.863787*	Miri Fm.	claystone	Mid-Late Miocene	Lambiase and Cullen, 2013
Tagap	Tag	*4.909600*	*114.854634*	Miri Fm.	claystone	Mid-Late Miocene	Lambiase and Cullen, 2013

Note that for the Lumapas limestone a younger age is proposed here based on SIS (see also Fig. 1).
*already published Sr-isotope data.

The samples were washed in an ultrasonic bath to remove any adherent sediment particles, and then were optically examined using a microscope. Suitable, unaltered areas were drilled with a *Dremel* diamond-bit hand-drill. Some of the calcareous samples were examined with X-ray diffraction (XRD) to assess their mineralogical composition (i.e., testing for original aragonite compositions, Fig. 2a) at the Universiti Brunei Darussalam, with a Shimadzu XRD-7000 diffractometer. Thick sections of part of an oyster shell from Subok (Sub-3) and a fragment of the Lumapas limestone (Lum-5) (Fig. 2b-i) were made at the Institute of Earth Sciences at University of Lausanne in Switzerland, and analyzed with the following optical methods: (1) Cathodoluminescence with an OPEA equipment model 8200 MkII, which allowed specific sampling of unaltered areas; (2) Raman spectroscopy to detect the mineralogy of the specimens. The subsampling was performed with an Olympus SZ61- NewWave MicroMill device. Prior to strontium isotope analyses, most of the calcareous samples were analyzed for minor and trace element (Sr, Mg, Mn, Fe), and stable oxygen and carbon isotope compositions to get further information about the habitat of the given taxa and/or the preservation state of the fossils. From some sites, samples with different preservation state were also analyzed in parallel in order to assess diagenetic pathways (e.g., recrystallized vs. pristine samples).

3.1. Strontium isotope analyses ($^{87}Sr/^{86}Sr$)

The sample powders were analyzed in two different laboratories, but with the same analytical method. A standard cation exchange resin (Eichrom Sr spec) was used to separate strontium with in columns washed with 3 N HNO_3. Sr was subsequently eluted with MilliQ® water. The $^{87}Sr/^{86}Sr$ ratios were either analyzed on a Finnigan MAT 262 thermal-ionization mass spectrometer at the Institute for Geology, Mineralogy and Geophysics of the Ruhr-University (Bochum, Germany), or by using a double focusing MC-ICPMS with a forward Nier–Johnson geometry (Thermo Fisher Scientific, Neptune TM) housed at the Centro Interdipartimentale Grandi Strumenti of Modena and Reggio Emilia (UNIMORE). For further details on sample preparation and analyzes see Li et al. (2011), Vescogni et al. (2014), and Lugli et al. (2017).

All the data were adjusted to a $^{86}Sr/^{88}Sr$ value of 0.1194 to correct for the instrumental fractionation. In the UNIMORE lab several NIST SRM 987 standards (between 6 and 13) were analyzed together with the samples and their 2 standard deviation were used to correct for instrumental bias to a value of 0.710248 (McArthur et al., 2001). Repeated analyses of the NIST SRM 987 had an external reproducibility (2sd) of 9 to 21 ppm, with higher variation relating to small standards analyzed with the micromill-sampled specimens (<1 mg). In the Bochum laboratory, USGS EN-1 and NIST SRM 987 were analyzed together with the samples. In our previous work, the long term value of USGS EN-1 were used for further normalization (see Kocsis et al., 2018: 0.709161 ± 0.000002; 2 s.e., n = 314), however to be consistent with the UNIMORE data, the long-term NIST SRM 987 of the Bochum laboratory (0.710240 ± 0.000002; 2 s.e., n = 423) were used to correct the $^{87}Sr/^{86}Sr$ ratios of the samples to the excepted value of 0.710248 (McArthur et al., 2001). This normalization results from 5 to 8×10^{-6} lower $^{87}Sr/^{86}Sr$ ratios when compared to the EN-1 corrected data. For most of the cases such differences are within the error of the standard deviation of multiple analyses from the same sites.

The measured $^{87}Sr/^{86}Sr$ ratios were compared to the look-up tables of McArthur et al. (2020), which is tied to the Geological Time Scale 2020 (Gradstein et al., 2020), and were used to derive numerical ages from the studied samples. Minimum and maximum ages were obtained by combining the statistical uncertainty (2 s.e.) of the mean values of the Sr-isotope ratios of the samples with the uncertainty of the seawater curve (Table 2).

3.2. Trace and minor element analyses

Prior to the Sr-separation, subset solutions from the larger calcareous samples were taken for measurements of Mg, Sr, Mn, and Fe concentrations. The elemental concentrations were determined on a Thermo Fisher Scientific iCAP6500 Dual View ICP-OES at the Bochum geochemical facilities, while a Perkin Elmer Optima 4200 DV ICP-OES was used at the University of Modena. The supernatant was diluted to 4 % w/w HNO_3 for the analyses, while an aliquot of the sample was further diluted to measure Ca concentration as well. The ICP-OES were externally calibrated with multi-element calibration standards in the concentration range from 1 ppb to 10 ppm for all the elements. Precisions were typically better than 5 % RSD (relative standard deviation) for Ca, Mg, Sr and Fe and better than 20 % for Mn. The data are expressed in ratios relative to Ca in mmol/mol (Fig. 4, Supplementary Table 1).

3.3. Stable isotope analyzes ($\delta^{18}O$ and $\delta^{13}C$)

A Gasbench II coupled to a Finnigan MAT Delta Plus XL mass spectrometer was used to analyze the carbonates for carbon and oxygen isotope compositions in the Stable Isotope Laboratory of University of

Table 2
Strontium isotope ratios of the studied materials and related SIS ages based on McArthur et al. (2020). Note that data with italics were not included in the final SIS age calculations (see text for details).

Samples and their origin					$^{87}Sr/^{86}Sr$	2SE	Age (My)	$^{87}Sr/^{86}Sr$	2SE	Age (My)		
							individual	Averages		min	mean	max
Belait syncline												
Lion King outcrop	LK	cc	Osteridae - bivalve	G	0.708877	0.000005	10.4	0.708877	0.000010	9.9	**10.4**	10.9
Tanjong Nangka	JT1-L2-1	cc	Osteridae - bivalve	G	0.708879	0.000005	10.3					
	JT1-L2-2	cc	Osteridae - bivalve	G	0.708887	0.000005	10.0					
	JT1-L2-3	ar	Sciaenidae - fish otolith	G	0.708882	0.000005	10.2					
	JT1-L1-1	cc	Osteridae - bivalve	G	0.708879	0.000005	10.3					
	JT1-L1-2	cc	Osteridae - bivalve	G	0.708833	0.000005	*12.3*					
	JT1-L1-3	cc	Osteridae - bivalve	G	0.708873	0.000005	10.5	0.708880	0.000016	9.5	**10.3**	11.0
Ikas Bandung	IB-1	cc	Pectenidae - bivalve	IT	0.708907	0.000007	9.3	0.708907	0.000012	8.5	**9.3**	9.8
Maraburong	MAR	cc	Osteridae - bivalve	G	0.708917	0.000006	8.9	0.708917	0.000010	8.0	**8.9**	9.4
Keriam	Ker	cc	Osteridae - bivalve	IT	0.708933	0.000004	7.9	0.708933	0.000009	7.2	**7.9**	8.7
Jalan Pak Bidang	JPB-1	cc	Osteridae - bivalve	IT	0.708946	0.000003	7.2					
	JPB-2	ap	*Hemipristis serra* - shark tooth	IT	0.708956	0.000005	6.8	0.708951	0.000012	6.5	**7.0**	7.9
Tutong beach (reworked)	TB-1	ap	*Otodus megalodon* - shark tooth	IT	0.708972	0.000005	6.4					
	TB-2	ap	*Hemipristis serra* - shark tooth	IT	0.708974	0.000005	6.3					
	TB-3	ap	cf. *Glyphys* - shark tooth	IT	0.708963	0.000005	6.6					
	TB-4	ap	Chelonid turtle bone	IT	0.708989	0.000006	6.1					
	TB-5	ar	Haemulidae - *Pomadasys* - fish otolith	IT	0.708941	0.000004	7.4	0.708968	0.000018	6.0	**6.5**	7.2
Berakas syncline												
Lumapas reef	Lum-1	cc	Turbo - gastropod operculum - recryst	G	0.708822	0.000005	*12.9*					
	Lum-2	cc	sea urchin spine - recryst	G	0.708828	0.000005	*12.6*	*0.708825*	*0.000010*			
	Lum-3	cc	Pectenidae - bivalve	IT	0.708875	0.000004	10.4					
	Lum-4	ar	Turbo - gastropod operculum	IT	0.708865	0.000005	10.8					
	Lum-5a	carb	micro-sampled shells tested with CL	IT	0.708870	0.000005	10.6					
	Lum-5b	carb	micro-sampled shells tested with CL	IT	0.708865	0.000005	10.8					
	Lum-5c	carb	micro-sampled shells tested with CL	IT	0.708880	0.000005	10.3	0.708871	0.000021	9.7	**10.6**	11.6
Jalan Subok	Sub-1	cc	Osteridae - bivalve	G	0.708813	0.000004	*13.5*					
	Sub-2	cc	Osteridae - bivalve	G	0.708820	0.000005	*13.0*					
	Sub-3		Osteridae - *Crassostrea* - bivalve									
	Sub-3a	cc	sub-sample with CL	IT	0.708808	0.000004	*13.9*	*0.708814*	*0.000021*			
	Sub-3b	cc	sub-sample with CL	IT	0.708833	0.000005	12.3					
	Sub-3c	cc	sub-sample with CL	IT	0.708842	0.000006	11.8	0.708837	0.000021	10.9	**12.1**	13.5
Dadap	Dad-1	cc	Osteridae - bivalve	IT	0.708877	0.000005	10.4					
	Dad-2	cc	Pectenidae - bivalve	IT	0.708870	0.000006	10.6	0.708874	0.000009	10.0	**10.5**	11.0
Tagap	Tag-1	cc	Osteridae - bivalve	IT	0.708879	0.000005	10.3					
	Tag-2	cc	Pectenidae - bivalve	IT	0.708879	0.000005	10.3	0.708879	0.000009	9.8	**10.3**	10.8
Sarawak, Malaysia												
Bekenu-Niah Road	Bek-1	cc	Pectenidae - bivalve	IT	0.708616	0.000006	17.7					
	Bek-2	cc	Pectenidae - bivalve	IT	0.708616	0.000007	17.7	0.708616	0.000012	17.5	**17.7**	17.9
Kg. Tengah	Ten-1	cc	Osteridae - bivalve	G	0.708696	0.000005	16.7			16.5	**16.7**	16.9
	Ten-2	cc	bivalve	G	0.708662	0.000006	*17.1*					
	Ten-3	cc	Osteridae - bivalve	IT	0.708663	0.000005	*17.1*	*0.708679*	*0.000023*			

Abbreviations: cc– calcite; ar – aragonite; ap – apatite; G – data from the German laboratory; IT – data from the Italian laboratory.

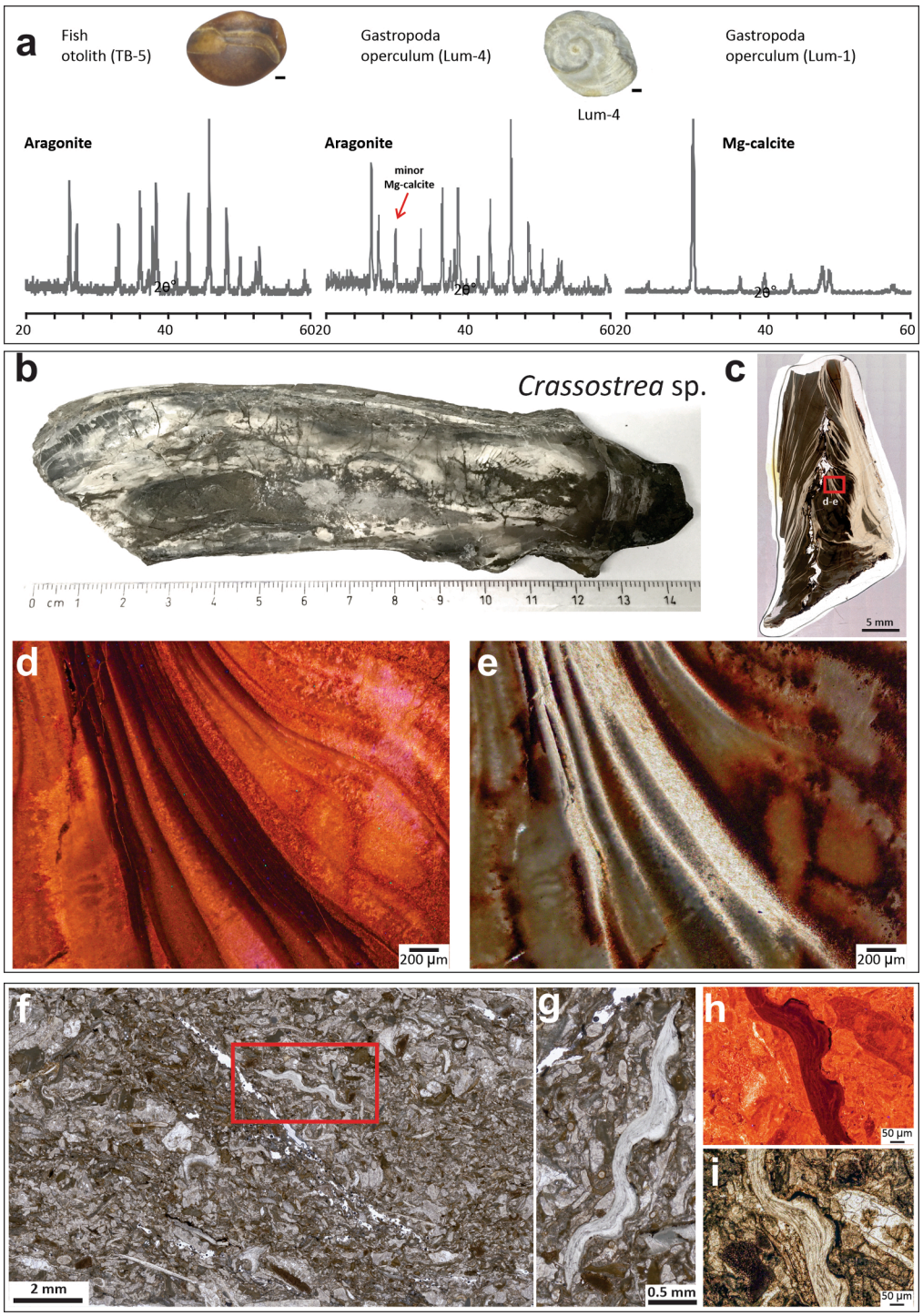

Fig. 2. (a) Selected X-ray diffraction patterns of originally aragonitic fossils. Modern operculum, fossil operculum (Lum-4); recrystallized operculum (Lum-1), and fish otolith (TB-5). (b-e) *Crassostrea* sp. from Subok (Sub-3): (c) Transmitted light (TL) image of a polished thick section of the shell. Note the thin, light colored, transparent, finely laminated layers, indicating well-preserved biomineral. The thick variable dark grey to opaque layers are micritic. Red rectangle marks close-up images with (d) cathololuminescence (CL) and (e) TL showing detailed shell structure. Shell layers transparent in TL, show a dark, dusky orange to mauve color banding under CL reflecting variable uptake of Mn^{2+} traces during growth, suggesting potential preservation for original trace element compositions and Sr-isotope ratios. The dark grey to brownish color in TL, show a mottled, variably orange to bright mauve CL activation, with irregular seams of small cements (e.g. bottom left). These parts of the shell are recrystallized and probably have a low preservation potential for in-vivo Sr-ratios. (f-i) Lumapas limestone (Lum-5): (f) TL-thin section scan and (g-i) close-up images of a small (3 mm long) bivalve fragment screened for SIS. (g, i) TL show well-preserved laminated biomineral texture for the shell. (h) CL of the shell yields a dark violet-mauve CL, resulting from the optical combination of the dark blue ($\lambda = 410–430$ nm) intrinsic luminescence of pure calcite and the yellow-orange CL ($\lambda = 600–650$ nm) of a low ($\ll$20 ppm) Mn^{2+} content. Very slight differences in the shade of violet are visible displaying the laminar biomineral texture. The remaining of the rock is composed of various bioclasts with a bright orange CL (>200 ppm Mn^{2+}), suggesting uptake of Mn^{2+} during diagenetic alteration in a reducing environment. (For interpretation of the references to color in this figure legend, the reader is referred to the web version of this article.)

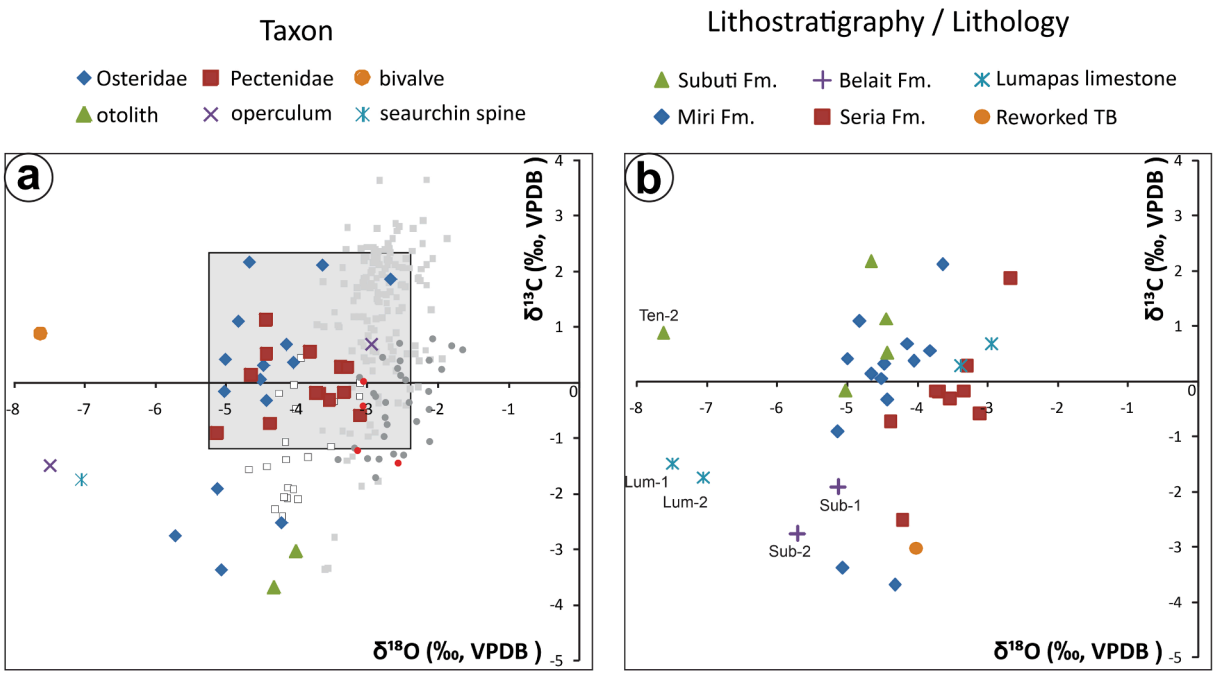

Fig. 3. (a-b) Oxygen versus carbon isotopic compositions of the studied calcareous remains according to the type of material (e.g., taxa) and to lithostratigraphy/lithology. Bruneian data from Ambug Hill (Kocsis et al., 2018) and Penanjong beach (Kocsis et al., 2021) are also included in these compilations. Modern (grey dots) and fossil (red dots) foraminifera data from Brunei (this study) and Miocene marine (grey square) and brackish (white square) gastropods from southeast Borneo (Reich et al., 2015) are displayed for comparisons. The grey rectangle covers geochemical range that considered reflecting local marine conditions and/or diagenetically less affected material (see text for discussion). (For interpretation of the references to color in this figure legend, the reader is referred to the web version of this article.)

Lausanne (UNIL), Switzerland (Fig. 3, Supplementary Table 1), following a method adapted after Spötl and Vennemann (2003). Beside the specimens for the Sr-isotope analyses, some modern and fossil foraminifera were also analyzed (Supplementary Table 2). The analytical precision for this method was better than ± 0.1 ‰ standard deviation as determined from multiple analyses of the in-house standard. The $\delta^{18}O$ and $\delta^{13}C$ values are expressed in the δ-notation relative to VPDB (Vienna Pee Dee Belemnite international reference standard).

4. Results

4.1. X-ray diffraction, cathodoluminescence (CL) and Raman spectroscopy

Two fish otoliths (JT1-L2-3 and TB-5) and two gastropod opercula (Lum-1 and Lum-4) originally composed of aragonite, were analyzed with XRD (Fig. 2a). Macro- and microscopic observation indicate that original structure for three of the specimens is preserved, whereas one of the opercula is clearly recrystallized (Lum-1). The three well-preserved specimens retained their original mineralogical composition, however with very minor amount of Mg-calcite in the operculum (Lum-4). In contrast, the second, recrystallized operculum is entirely composed of Mg-calcite (Lum-1).

One oyster shell from Subok (Sub-3) and a small calcite shell (Lum-5) within a limestone block from Lumapas were examined in CL (Fig. 2 d, h). The oyster shell is made of a layered structure with two distinct, often inter-fingered layers: (1) Finely laminated layers, transparent in TL (transmitted light), composed of fibres or lamellae of approximately 15 μm size that are well organized in shingles, which are oriented obliquely to the growth lines of the shell. Under CL they show a low, dusky orange to mauve color banding, reflecting variable uptake of Mn^{2+} traces during growth, hence, they could potentially have preserved original trace element compositions and Sr-isotope ratios. (2) Variable mottled dark grey to brownish areas in TL, with areas showing faint phantoms of a "prismatic" structure, replaced by fine micrite, irregularly stained by Fe-hydroxides that gives the rusty tint to the shell (Fig. 2 c,e). In CL these layers reveal a mottled, variably orange to bright mauve luminescence (Fig. 2 d), showing irregular seams of small cements. The mottling is also seen on the TL images where the original biogenic structure is partly destroyed (Fig. 2 e). This part of the shell is diagenetically altered and may have exchanged with Sr and other trace element with the pore water during diagenesis.

The small Lumapas specimen (Lum-5, length: 3 mm 5 by 0.5 mm, Fig. 2 f-g) is most possibly a bivalve shell whose cross section shows a laminated texture reminiscent of a laminar calcite biomineral (detected by Raman spectroscopy). It is transparent in TL because of its fibrous texture. The CL of the shell is dark violet-mauve (Fig. 3h) resulting from the optical combination of the dark blue (λ = 410–430 nm) intrinsic luminescence of pure calcite, and yellow-orange (λ = 600–650 nm) of a low (≪20 ppm) Mn^{2+} content (Sommer, 1972; Baumgartner-Mora and Baumgartner, 1994). Very slight differences in the shade of violet are visible displaying the laminar biomineral texture. The remaining of the rock is composed of various bioclasts with a bright orange CL (>200 ppm Mn^{2+}), suggesting uptake of Mn^{2+} during diagenetic alteration in a reducing environment (Cazenave, 2003).

4.2. Stable isotope compositions

Twenty-seven calcareous samples were analyzed for stable carbon and oxygen isotopic compositions. The $\delta^{18}O$ values have a range between −7.6 and −2.7 ‰, with an average of −4.7 ± 1.2 ‰, while the $\delta^{13}C$ values have a range from −3.7 to 2.2 ‰ with an average of −0.3 ± 1.7 ‰. Taxonomy and the range of values for each locality are illustrated in Fig. 3a-b. Modern large benthic foraminifera in the Brunei region had an average $\delta^{13}C$ and $\delta^{18}O$ of −2.6 ± 0.4 ‰ and −0.3 ± 0.7 ‰ (n = 30), respectively (Supplementary Table 2). Some fossil foraminifera were also analyzed from Ambug Hill and the respective mean values are −2.9 ± 0.3 ‰ and −0.8 ± 0.7 ‰ (n = 4) (Supplementary Table 2).

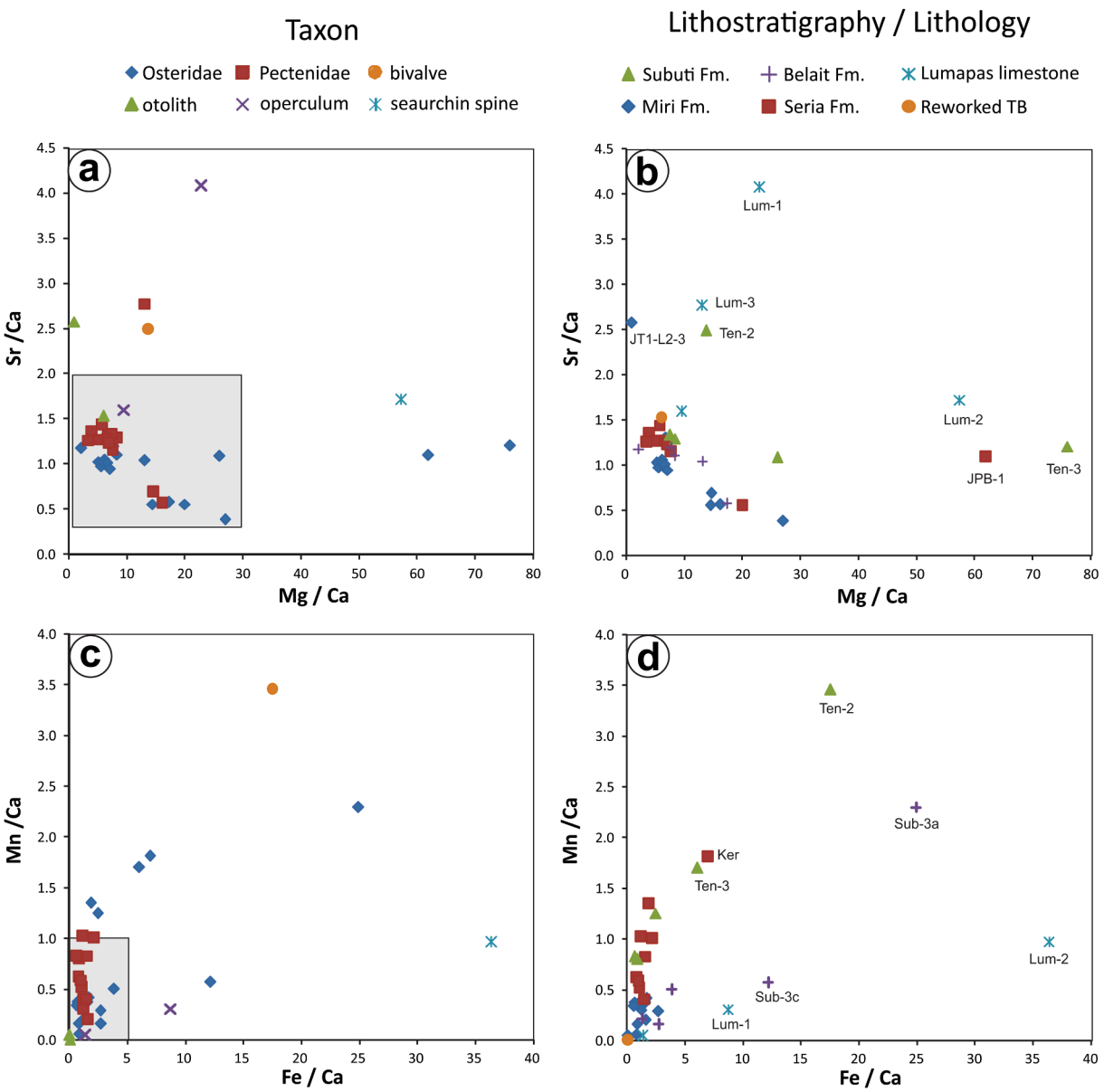

Fig. 4. (a-b) Mg/Ca vs Sr/Ca, and (c-d) Fe/Ca vs Mn/Ca ratios of the studied calcareous remains according to the type of material (e.g., taxa) and to lithostratigraphy/lithology. The grey rectangles cover geochemical range that considered reflecting local marine conditions and/or diagenetically less affected material (see text for discussion). Note the outlier Lumapas samples (Lum-1 and 2) that are clearly recrystallized (see also Fig. 2a and Fig. 3).

4.3. Trace and minor element compositions

Of the 33 carbonates, 30 were analyzed for their trace elemental compositions, only the very small Lumapas carbonate samples were excluded. The data are plotted in terms of taxa and locality in Fig. 4a-d. The Mg/Ca ratios have a range between 0.9 and 76 with the majority of the samples below 25, and only three samples gave values higher than 50 mmol/mol. The Sr/Ca ratios are from 0.4 to 4.1 mmol/mol with the highest frequencies around 1 and 1.2 mmol/mol. The Fe/Ca ratios vary between 0.03 and 36.4 mmol/mol, with more than two-thirds of the samples below 4 mmol/mol. The Mn/Ca ratios have a range from 0.01 to 3.5 mmol/mol among the samples, with most of them are below 1–1.5 mmol/mol.

4.4. Strontium isotope ratios and related ages

Thirty-eight $^{87}Sr/^{86}Sr$ analyses are provided here from thirteen localities (Table 2). Generally, one to three samples per locality were analyzed except for the three sites Tanjong Nankga (JT1), Subok (Sub), and Lumapas (Lum), where more samples and subsamples were measured. In addition, several samples were measured from the reworked Tutong beach site (TB). 24 analyses were done on thick calcite shells of oysters and scallops among which three are subsamples with a different CL response of the Sub-3 sample. In addition, three micro-sampled carbonate shells (subsampled based on CL appearance, Lum-5a-c) and two clearly recrystallized calcite specimens (sea urchin spine: Lum-2 and a gastropod operculum: Lum-1) were analyzed from the Lumapas limestone. The rest are one unidentified bivalve from Tengah (Ten-2), 3 XRD-tested aragonite samples (otoliths: JT1-L2-3 and

TB-5, and an operculum from Lumapas: Lum-4), and 5 bioapatite (teeth: TB-1–3 and bone TB-4). The overall data have a range from 0.708616 to 0.708989 that can be translated to a mean age range of 17.7 to 6.1 million years, when compared to the open ocean Sr-isotope evolution curve (McArthur et al., 2020). The averages for each locality without outliers and obviously altered data are also shown in Table 2 and plotted in Fig. 5 with compound errors accounting for the spread of the data, for sub-set measurements, and their fits to the Sr-isotope curve.

5. Discussion

5.1. Preservation of the fossils

Stable oxygen and carbon isotope compositions of seawater vary in much narrower ranges than freshwater, where $\delta^{18}O$ is usually lower relating to oxygen isotopic fractionation during evaporation/condensation processes, while $\delta^{13}C$ of dissolved inorganic carbon (DIC) is also lower due to the influence of terrestrial derived organic matter (e.g., Lohmann, 1988). In terms of trace element chemistry, seawater generally has higher Sr and Mg, and lower Mn and Fe concentrations than brackish and freshwater (White, 1998; Bruland and Lohan, 2003; Gaillardet et al., 2003). All these parameters can help assessing environmental conditions in coastal shallow marine and estuarine settings, such as we investigated here. These parameters could also cause difficulties to define cut-off values for unaltered samples before Sr-isotope analyses. During diagenesis the fossils interact with pore fluids in the sediment and depending on the conditions, lower $\delta^{18}O$ and/or $\delta^{13}C$, while loss of Sr and Mg, and addition of Fe and Mn might be expected in calcareous remains (e.g., Brand and Veizer, 1980). At surface conditions aragonite is thermodynamically less stable than calcite (e.g., Plummer and Busenberg, 1982; Bischoff et al., 1987), hence originally aragonitic fossils (otolith, gastropod remains) were always tested here with XRD. In case of bioapatite, rapid incorporation of rare earth elements (REE) and U from the early burial environment is well-known (e.g., Trueman and Tuross, 2002), which process might also modify slightly the Sr content and hence the Sr-isotope ratio. For this reason, well-crystallized hard biominerals, such as tooth enamel/enameloid, were used in our study, in which material the chance of diagenetic overprint is much reduced (e.g., Zazzo et al., 2004).

Few samples from two Bruneian sites, the Lumapas limestone and the Subok oyster mounds, were screened here with CL, while from the rest of the localities all the calcareous remains were analyzed for stable oxygen and carbon isotope, and trace and minor element compositions. These geochemical data are plotted following taxonomy and lithostratigraphy in Figs. 3-4, together with earlier published data from Brunei (Kocsis et al., 2018, 2021). Bioapatite samples were analyzed only for $^{87}Sr/^{86}Sr$ ratio (JPB and TB, see Table 2).

5.1.1. Stable isotope composition of carbonates

The data show a relatively large spread for both isotope systems. However, the scallops (Pectenidae) have a more restricted range, while the oysters (Osteridae) have a larger range, especially in $\delta^{13}C$ (Fig. 3a). Most of the $\delta^{18}O$ values plot in a relatively narrow range though, between about −5 and −3 ‰ with clear outliers such as one of the Tengah bivalves (Ten-2) and the recrystallized remains from the Lumapas limestone (Lum-1 and Lum-2) (Fig. 3a). In terms of $\delta^{13}C$, most of the data vary between −1 and 2 ‰, with notable exceptions being the fish otoliths and some oysters. The low $\delta^{13}C$ values in the fish otoliths are best explained by vital effect (e.g., Kalish, 1991; Thorrold et al., 1997). In contrast, the larger variation in the oyster data is linked to the habitat conditions as they can live in intertidal environments and in estuaries where brackish conditions and larger contribution of terrestrially derived DIC is expected (e.g., Surge et al., 2001; Mouchi et al., 2020). As their $\delta^{18}O$ is rather similar to the majority of the samples, the low $\delta^{13}C$ may reflect a close position to mangrove habitats that are/were common in coastal regions in Borneo.

Modern large benthic foraminifera from Brunei's shallow marine sites have similar $\delta^{13}C$ values and 2–3 ‰ higher $\delta^{18}O$ values (Fig. 3a, see Supplementary Material Table 2). Miocene marine and brackish water gastropods from southeast Borneo (-3.6 to −1.9 ‰, Reich et al., 2015) have a wider $\delta^{13}C$ range and slightly higher $\delta^{18}O$ values. These differences can be linked to different vital effects among these organisms (i.e., biomineralization) and/or to different environmental and climatic conditions (e.g., higher ambient temperature). Interestingly, both oysters and scallops have relatively higher $\delta^{18}O$ values in the younger Seria Formation than in the Miri Formations (Fig. 3b). This may link to globally recognized trends in the Late Miocene that reflect decreasing ambient temperature and/or the related accumulation of ice in the polar regions (e.g., Zachos et al., 2001).

In summary, the clear outliers need to be considered with care when SIS is applied, while the obviously recrystallized samples may still be useful in the sense of being indicators of the direction of diagenesis, and hence possible offsets from the Sr-evolution curve.

5.1.2. Trace and minor element compositions of the calcareous remains

These data show large variation among the samples. The Mg/Ca and Sr/Ca ratios are largely in the reported ranges for oysters (Surge and Lohmann, 2008; Ullmann et al., 2013) and scallops (Freitas et al., 2006, 2012), however some specimens show relatively higher Mg and lower Sr concentrations (Fig. 4a), which may indicate either strong local influence (e.g., Mouchi et al., 2018) or alteration. The diagenetic overprint is evident for the two recrystallized fossils of the Lumapas limestone (Lum-1 and Lum-2), but partial exchange might be expected for other specimens with outlier values such as $Mg/Ca > 30$ and $Sr/Ca > 2$ (Fig. 4a-b).

In terms of the Fe/Ca and Mn/Ca, some samples have extremely high values that are a clear indication of a post-mortem, diagenetic incorporation of Fe and Mn (Fig. 4c-d). Wide range of cut-off Fe and Mn values were suggested to consider a calcareous sample suitable for SIS (see Schneider et al., 2009 and references therein). In the case of our Bornean samples, some of them were sampled from coquina beds that are often cemented by siderite (Abdul Hadi and Astin, 1995; Kocsis et al., 2018), while some of the bivalve shells also contained pyrite inclusions in their shell. Moreover, when these beds and fossils are exposed to tropical weathering the reduced Fe-minerals oxidize to form iron oxide/hydroxides that can precipitate within the cracks of the shells. The fossils were always carefully examined before being sampled, and altered parts with secondary minerals were avoided. Nevertheless, the observed minerals indicating suboxic-anoxic early burial conditions and Fe and Mn could have been incorporated in the shells' microstructure during early exchange. However, these elements could have been also available in somewhat higher concentration in the coastal environment and higher *in-vivo* values could not be directly rejected. Whether and to which extent the early diagenetic incorporation of these elements affect the Sr-isotope ratios is difficult to assess (e.g., Schneider et al., 2009). Mn/Sr ratio < 2 was suggested as another indicator for pristine $^{87}Sr/^{86}Sr$ ratios (e.g., Jacobsen and Kaufman, 1999), which would be valid for most of our samples as well (Supplementary Table 1). To sum up, in the view of the data range, samples with $Fe/Ca > 5$ and $Mn/Ca > 1$ have to be interpreted with caution when it comes to SIS. Finally, a low concentration of Fe and Mn is also not a definite evidence for unaltered samples (e.g., Jones et al., 1994; McArthur et al., 1994; Wierzbowski and Joachimski 2007; Frijia et al., 2015).

5.1.3. Strontium isotope ratios

The range of Sr-isotopic ratios among multiple Sr-isotope analyses from the same bed or rock units can give further insight about the preservation state or the origin of the fossils (e.g., McArthur et al., 2020). For the localities where only one analysis was carried out we relied on other screening methods and/or the sites' stratigraphic position relatively to other sites with age estimates derived from literature. In the sites where two specimens were analyzed, the average $^{87}Sr/^{86}Sr$

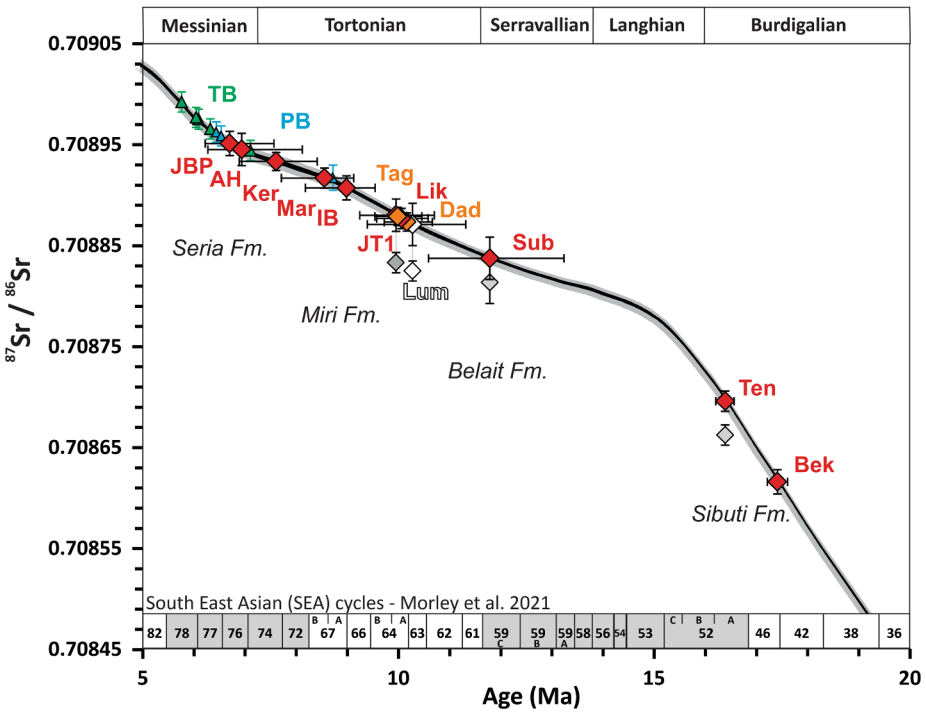

Fig. 5. $^{87}Sr/^{86}Sr$ ratios plotted on the open marine Sr-isotope evolution curve (McArthur et al. 2020). The curve displayed with its 95% confidence intervals (grey band). Red and orange diamonds reflect data from well-preserved material, which were directly placed on the Sr-isotope curve, while the grey diamonds with diagenetically altered Sr-ratios that are below the curve at their respective site (JT1, Sub, Ten). The same goes for the Lumapas limestone data (Lum), but they are marked with white diamonds as these data indicate younger age than expected from previous studies (Fig. 1d). Reworked material marked with green (Tutong beach – this study) and blue (Penanjong beach – Kocsis et al., 2021). Note that for these samples all individual analyses are plotted and most of them were probably originated within the younger cycles of the Seria Fm.. Along the x-axis the South East Asian (SEA) transgressive–regressive cycles are also shown after Morley et al. (2021). (For interpretation of the references to color in this figure legend, the reader is referred to the web version of this article.)

ratios were always within the analytical error (JBP, Dad, Tag, and Bek), hence these data could be used more confidently for SIS, even if some samples have somewhat lower Sr/Ca (e.g., Tag-1) or higher Mg/Ca (e.g., JPB-1) ratios.

Three mollusk shells were analyzed from the Tengah site (Sibuti Formation) and their average $^{87}Sr/^{86}Sr$ value varies within a relatively narrow range (0.708674 ± 0.000019). However, one of the specimens (unidentified bivalve: Ten-2) has an extremely low $\delta^{18}O$ values (Fig. 3a) and relatively high Fe and Mn contents. Meanwhile, the other two fossils have higher Mg/Ca ratios. Hence, even if, one of the samples appears likely to have been altered, it seems that this did not affect much the $^{87}Sr/^{86}Sr$. Nevertheless, the shift to lower $^{87}Sr/^{86}Sr$ ratio is obvious, hence the sample with the highest value are those used for SIS, (Figs. 3-4, Supplementary Table 1).

From the Subok site (Belait Formation) three oysters were analyzed, one with three subsamples with different CL response (Sub-3a-c). Although the spread of $^{87}Sr/^{86}Sr$ is fairly narrow (0.708823 ± 0.000014), the sample with high luminescence (Sub-3b-c) also have the lowest Sr-isotope ratio followed by two bulk shell samples (Sub-1–2), then the ones with low luminescence have the highest Sr-isotope ratios (Sub-3a). Regarding trace element concentrations in the micro-sampled shell, the CL observation is confirmed (Supplementary Table 1). Stable isotope compositions analyzed from the bulk samples (Sub-1–2) are also slightly different compared to the majority of the samples (Fig. 3a-b). Therefore, the better preserved two samples with the lowest luminescence and highest $^{87}Sr/^{86}Sr$ ratios are suggested here to be used for SIS.

From the Tanjong Nangka locality (Miri Formation) four oyster shells and one fish otolith have quite consistent $^{87}Sr/^{86}Sr$ ratios with an average value of 0.708880 (±0.000005), however a fifth oyster yielded much lower value (0.708833). The trace element and stable isotope compositions of these samples do not actually help to screen out this specimen. Two of the other oysters however, yielded lower $\delta^{13}C$ (-3.4 and −3.7‰), but it appears that once again this did not affect their Sr-isotopic ratios. The locality is probably best represented by the average of the five specimens, while the outlier sample is either an altered or reworked specimen.

From the Lumapas limestone, five fossils were tested, one with three subsamples where CL analyses indicated good preservation (n = 7). Two samples are clearly recrystallized based on microscopic observation, and they also have very low $\delta^{18}O$ values (Fig. 3a-b) and high Mg/Ca and Fe/Ca ratios. These samples have an average $^{87}Sr/^{86}Sr$ ratio of 0.708825 (±0.000004). In contrast, the two other macro-samples display original shell structure, and the aragonite specimen retained most of its mineralogical composition (Fig. 2a). Their stable isotope and trace element compositions also support good preservation (Figs. 3-4). In relation to Sr-isotope analyses, they have an average $^{87}Sr/^{86}Sr$ of 0.708870 (±0.000007), which is higher than those of the recrystallized specimens. The three micro-samples tested only by CL yielded very similar $^{87}Sr/^{86}Sr$ ratios (0.708872 ± 0.000006) to the well-preserved specimens. Therefore, the average of the five concurring analyses is used for SIS.

To sum up, it must be pointed out, that whenever we observe a major or minor shift with respect to a presumably unaltered $^{87}Sr/^{86}Sr$ ratio among our investigated samples, it is always going towards lower Sr-isotopic ratios. The evolution of the open marine Sr-isotope ratios displays an increasing trend since the Oligocene which is interpreted as an increasing proportion of crustal (radiogenic) ^{87}Sr input (e.g., McArthur et al., 2020). The observed shifts towards less radiogenic ratios in our samples (suggesting older ages) could relate to exchange with burial fluids which are either (1) affected by dissolution of older calcareous remains in the sedimentary successions, or (2) alteration of mantle-derived detrital minerals.

5.2. SIS dating

The Sr-isotope data of unaltered fossils were used here to obtain numerical ages via comparison with the global open marine Sr-evolution curve (McArthur et al., 2020) (Fig. 5, Table 2). The largest error is always applied to calculate the age that could be related to analytical uncertainties (sample or multiple standards) or standard deviation for site averages, and to the 95% confidence limits of the Sr-evolution curve itself. The data are mainly discussed following lithostratigraphic units.

The obtained ages can be further compared to the recently introduced South East Asian (SEA) transgressive–regressive cycles based on the sequence biostratigraphic framework introduced by Morley et al. (2021). Quantitative biostratigraphic data from over 100 petroleum wells were reviewed in northern Borneo within a chronostratigraphic

framework considering global glacio-eustatic sea level and stable isotope variations. Recognizing these SEA cycles in onshore small-scale outcrops, where biostratigraphic data are sparse is usually difficult, however the SIS data can give further insight.

Sibuti Formation – This is a succession of clay-shales with siltstone, marlstone, and limestone intercalations that are often rich in fossils. The rocks can be studied in the region of Bekenu town, from where Wannier et al. (2011) reported fossiliferous beds along road cuts towards the Niah caves and near Kampong Tengaha site west of Bekenu. These outcrops were targeted here with SIS, and one of the Bekenu road outcrops has an age of 17.7 ± 0.2 My, while the Tengah site is 16.7 ± 0.2 My old. These ages would correlate with the SEA 46 and 52A cycles, respectively (Morley et al., 2021). The Burdigalian ages fit in the overall range of Early Miocene to early Middle Miocene given for the Sibuti Fm (Liechti et al., 1960). Further northeast from the investigated sites, near Kpg. Opak, a limestone series crops out and the biostratigraphy indicates a rather younger age of Middle Miocene for the top part of the Sibuti Fm (Simon et al., 2014). The actual relation of this site to our investigated localities is difficult to assess as the region is affected by many faults and the layers are tilted. The Tengah and Bekenu road outcrops dip towards south – southeast, while the Opak Limestone to northwest. Nevertheless, the Opak Limestone most probably represents a younger cycle within this formation.

Belait Formation – The rocks are dominantly sandy and silty with occasional clay intercalations. The sediments often display ripple marked sand they frequently contain rich trace fossil assemblages (e.g., James, 1984; Fiah and Lambiase, 2014). Some authors consider a strong fluvial influence in this sedimentary succession (e.g., Tate, 1974; Sandal, 1996), while others interpreted variation between wave- and tide-dominated deltaic environment (e.g., Lambiase et al., 2003; Lambiase and Cullen, 2013). In these sediments the preservation potential of any calcareous remains is very low. Extensive exposure of the sediments can be studied along sandy ridges in the southern part of the Berakas syncline, but these rocks are also exposed along the coastline (e.g., Meragang beach). Recently due to housing development a ~ 6-meter-thick, fossiliferous (mollusks, crustaceans, amber) clay succession was discovered in Subok (Fig. 1; Kocsis et al., 2020; Roslim, 2021), which opened the opportunity to obtain numerical age for this site with SIS. The Sr-isotope ratios correspond to an age of 12.1 + 1.4/-1.2 My (Serravallian). This age can be correlated with the ~ SEA 59B-C depositional cycles of Morley et al., 2021 (Fig. 5).

The sediments of the Belait Fm were deposited from late Early Miocene till the latest Miocene (Liechti et al., 1960; Wilford, 1961) and the layers in the Subok area are considered to be of Middle Miocene age (e.g., Lambiase and Cullen, 2013). Therefore, the SIS age concur with previous suggestions, but also provides a more precise numerical age for this fossiliferous site. The discovered fauna at Subok clearly indicate stronger marine influence within the Belait Fm, but the frequent presence of lignite beds (e.g., about 15 m up section) indicates nearby estuarine, brackish conditions. Compared to other fossil-rich marine sites in Brunei, here bivalves, generally with marine habitat dominate. However large oysters (*Crassostrea*) can also live under brackish conditions. Marine gastropods are present (e.g., Conidae) but much rarer, while fish remains are also very sporadic (few teeth) compared to other localities. These may link to somewhat special habitat conditions (e.g., higher variability in salinity), nevertheless the obtained SIS age fit the general age range of this region.

Lumapas Limestone – The only carbonate rocks that occur in Brunei were mapped and described by Wilford (1961), who considered these sediments as embedded within the Belait Formation. The limestone represents a shallow marine environment with many large scleractinian corals, with occasional mollusks and echinoderms. Briguglio et al. (2017) reported the presence of miogypsinid foraminifera that may indicate a late Early Miocene age. This age concurs with the age assumption of the siliciclastic rocks of the Belait Fm cropping out nearby, based on their lower position in the sedimentary succession. Our Sr-isotope data, however, yielded a younger age of 10.6 ± 1 My (Tortonian) (Fig. 5) contrasting with the previous data. Both the surrounding sandy-silty rocks of the Belait Fm and the limestone are tilted towards NW, however it seems that the limestone dips with a somewhat lower angle (40-48°) than the Belait rocks (50-52°). Unfortunately, the contact between the limestone and the Belait Fm is not exposed, but the slight differences in the dip angles may reflect either an unconformity or can be the genuine contact of the reefal body. In the view of the SIS age, the coral reef could have grown on the already lithified and tilted Belait rocks. Such situation can be also observed today in the modern environment few kilometers off the coast of Brunei at the Pelong Rock, where the modern reef builds on tilted Middle-Upper Miocene successions (Goeting et al., 2018). Considering the possible presence of miogypsinid forams in the limestone (Briguglio et al., 2017) would disagree with our SIS age as this taxon is known to be existed only till the late Serravallian (early N13 Planktonic Zone, > ~12 Ma, BouDagher-Fadel and Price, 2013). Therefore, either (1) the preliminary reported large benthic foraminifera need further taxonomic clarification; or if they are indeed miogypsinids then (2) they are either reworked from older rocks; or (3) the taxon in fact may have survived until the early Late Miocene as a sort of refugium. An alternative solution would be the complete rejection of the SIS ages with reasoning as strong alteration. However, based on the Sr-isotope data of the clearly recrystallized and altered specimens, the diagenetic trend would suggest an opposite trend (i.e., the younger the samples the less altered they are). Therefore, here we accept the age of 10.6 ± 1 My (Tortonian) for the Lumapas limestone, which would indicate deposition during the SEA 62–63 cycles (Morley et al., 2021).

Miri and Seria formations – The rocks of the older Miri Formation crop out in both sides of the Jerudong anticline (Fig. 1). In the eastern side a rather narrow range of clay-rich succession occurs that can be locally fossiliferous. Laterally (S-SE) and up section more sandstone beds are found and the rocks grades into the deposits of the Belait Fm. The two investigated localities are approximately on the same strike and accordingly they yielded very similar SIS ages, 10.5 ± 1 My (Dad) and 10.3 ± 0.5 My (Tag), corresponding to early-middle Tortonian (Fig. 5). In the eastern side, the succession starts with almost vertical sandstone horizons (Lion King – LK outcrop), with few clayey layers, one of those full of mollusk molds, with occasional preservation of thin oyster shells. Moving away from the core of the anticline the inclination of the beds decreases and more distinct parasequences appear with fossiliferous claystone base and coarsening up section with erosional top. The series gets younger towards NE, and with increased proportion of sand the Seria Fm follows with even lower dip angles. The Miri Fm localities near the core of the Jerudong anticline yielded SIS ages of 10.4 ± 0.5 My (LK) and 10.3 + 0.7/-0.8 My (JT-1) that are comparable with the eastern side. However, based on the relative distance of the two sites older age might have been expected for the Lion King site (LK). The area is tectonically active and several small faults have been detected next to the Jerudong anticline (Back et al., 2005) that may explain exposure of older stratigraphic intervals. Towards NW the other sites show the expected younging trend with SIS ages of 9.3 + 0.5/-0.8 My (IB) and 8.9 + 0.5/-0.9 My (Mar), where the trend continues in the Seria Fm where ages of 7.9 + 0.8/-0.7 My (Ker) and 7.0 + 0.9/-0.5 My (JPB) are found. The latter date is similar to the nearby Ambug Hill locality (7.2 + 1.2/-0.6 My; Kocsis et al., 2018).

The SIS analyses confirmed the general Late Miocene ages of these formations in Brunei (Wilford, 1961; James, 1984), however indication of absolute ages or detailed biostratigraphic data are rare in the literature. Age isolines can be found in the map of Back et al. (2005: Fig. 3) west of the Jerudong anticline with ~ 12 Ma and ~ 10.6 Ma. These ages are derived from palynology without further explanation in the text. Our Tanjong Nangka site (JT-1) is situated just between these isolines, and the related SIS data (10.3 ± 0.8 Ma) overlap with the younger isoline age of Back et al. (2005). Other biostratigraphic data come from the younger part of the Seria Fm, where calcareous nannoplankton data (NN11) were reported from the Ambug Hill (Kocsis et al., 2018), that

also concur with the SIS ages. In terms of the sequence biostratigraphic framework, the ages of the Miri Fm sites can be linked to ~ SEA 62–67, while the Seria Fm sites to the SEA 74–77 cycles of Morley et al., (2021).

Reworked samples at Tutong beach – Vertebrate remains, mainly shark teeth and turtle shell fragments, are often washed up near Tutong along a 2–3 km stretch of the shoreline. A similar situation could have existed at Penanjong beach (0.5–1 km northeast) before the construction of the coastal protection line (Kocsis et al., 2021). Even if the fauna is mixed and reworked, a fairly consistent and a relatively narrow age range was obtained (6.1–7.4 My, Messinian – late Tortonian). These ages match with that of the nearby localities of the Seria Formation (Ambug Hill – Kocsis et al. 2018; JPB – this study) and indicate origin from these types of hinterland rocks. These outcrops also yielded many *in-situ* shark teeth, otoliths, and also occasional turtle remains (Kocsis et al., 2019, 2021; Roslim et al., 2020). It may be worth mentioning that the bioapatite data also gave a somewhat younger age than the single otolith (TB-5) measurement, which may be taken assign of a diagenetic offset, especially in the case of the turtle bone sample (TB-4) (i.e., tooth enameloid data are more robust). However due to the mixed nature of these samples it is difficult to cross-check such a shift. Nevertheless, to sum up, the older ages fit well with the SIS ages obtained here from the younger beds of the Seria Formation supporting the stratigraphic origin of these fossils.

6. Conclusions

Thirteen fossil-rich coastal shallow marine sites in Brunei and Sarawak (Malayisa) were dated with strontium isotope stratigraphy (SIS). The selected calcareous samples were screened with different methods in order to help detect altered specimens, but also shed light on ecological habitats for the unaltered samples. For example, oysters (Osteridae) yielded higher variation in $\delta^{18}O$ than scallops (Pectenidae), probably indicating more various habitats from coastal to estuarine environment. Interestingly, these taxa together show time related shift with overall higher $\delta^{18}O$ values in the younger samples (Miri vs. Seria Fm) that may reflect global cooling trend and related ice-volume effect.

The well-preserved samples were used for SIS and the following ages were obtained for the studied fossil-rich sites: 17.7 ± 0.2 My and 16.7 ± 0.2 My (Burdigalian) in the Sibuti Formation in Sarawak, 12.1 + 1.4/-1.2 My (Seravallian) in the Belait Fm in Brunei, from 10.5 ± 1 My to 8.9 + 0.5/-0.9 My (Tortonian) in Miri Fm sites in Brunei, and 7.9 + 0.8/-0.7 My and 7.0 + 0.9/-0.5 My (Tortonian-Messinian) from the Seria Fm. The age range (6.1 – 7.4 My) obtained from reworked vertebrate remains near Tutong indicate an origin from the deposits of the Seria Fm. The obtained numerical ages fit with the large stratigraphic framework reported for the region in the literature but help to precisely date for the first time such important sites. The Lumapas limestone in Brunei is the only exception, as the obtained SIS age (Tortonian, 10.6 ± ~1 My) contradicts with ages assumed from stratigraphic position (~late Burdigalian) and confirmed presence of miogypsinid foraminifers which should be already extinct during the Tortonian. The clearly altered samples from this site with lower $^{87}Sr/^{86}Sr$ ratio would point to older SIS age, hence such diagenetic trend would support the younger age scenario. In this case, the reported occurrence of miogypsinids either (1) need taxonomical revision, or (2) their presence is due to reworking, or (3) alternatively one may propose longer time span for this taxon as known so far. The young age would also point to unconformity between the Belait rocks and the limestone, however better exposure is needed to confirm this.

CRediT authorship contribution statement

László Kocsis: Conceptualization, Investigation, Data curation, Writing – review & editing, Visualization. **Antonino Briguglio:** Investigation, Resources, Writing – review & editing. **Anna Cipriani:** Methodology, Data curation, Writing – review & editing. **Gianluca Frijia:** Methodology, Data curation, Writing – review & editing. **Torsten Vennemann:** Methodology, Data curation, Writing – review & editing. **Claudia Baumgartner:** Methodology, Data curation, Writing – review & editing. **Amajida Roslim:** Investigation, Resources.

Declaration of Competing Interest

The authors declare that they have no known competing financial interests or personal relationships that could have appeared to influence the work reported in this paper.

Acknowledgements

We are grateful to Peter Baumgartner for his inputs on an earlier version of the manuscript. We appreciate the help of Han Raven for the identification of the Subok oysters. Constructive comments on the manuscript by the two reviewers, Masatoshi Sone and an anonymous one, are much appreciated. To some extent the research was supported by university research grants (UBD/PNC2/2/RG/1(325&326), UBD/RSCH/1.4/FICB F(b)/2019 /023).

Appendix A. Supplementary data

Supplementary data to this article can be found online at https://doi.org/10.1016/j.jseaes.2022.105213.

References

Abdul Hadi, A.R., Astin, T.R., 1995. Genesis of siderite in the Upper Miocene, offshore Sarawak: Constraints on pore fluid chemistry and diagenetic history. Bull. Geol. Soc. Malays. 37, 395–413.
Back, S., Morley, C., Simmons, M., Lambiase, J., 2001. Depositional environment and sequence stratigraphy of Miocene deltaic cycles exposed along the Jerudong anticline, Brunei Darussalam. Journal of Sedimentary Research 71 (6), 913–921.
Back, S., Tioe, H.J., Thang, T.X., Morley, C.K., 2005. Stratigraphic development of synkinematic deposits in a large growth-fault system, onshore Brunei Darussalam. Journal of the Geological Society, London 162 (2), 243–257.
Baumgartner-Mora, C., Baumgartner, P.O., 1994. Shell structure of fossil foraminifera studied by cathodoluminescence. Microscopy and Analysis 3, 35–38.
Beets, C., 1947. On probably Pliocene fossils from Mahakkam delta region, East Borneo, and from Dessah Garoeng (Lamongan). Java. Geol. & Mijnbouw 9 (10), 193200.
Beets, C., 1983. Miocene molluscs from Muara Kobun and Pulu Senumpah, Sangkulirang Bay, Northern Kutai (East Borneo). Scripta Geol. 67: 121, p i 1.
Bellwood, D.R., Renema, W., Rosen, B.R., Gower, D., Johnson, K., Richardson, J., Rosen, B., Ruber, L., Williams, S., 2012. Biodiversity hotspots, evolution and coral reef biogeography: a review. In: Gower, D., Johnson, K., Richardson, J., Rosen, B., Ruber, L., Williams, S. (Eds.), Biotic Evolution and Environmental Change in Southeast Asia. Cambridge University Press, Cambridge, pp. 216–245.
Bischoff, W.D., Mackenzie, F.T., Bishop, F.C., 1987. Stabilities of synthetic magnesian calcites in aqueous solution: Comparison with biogenic materials. Geochim. Cosmochim. Acta 51, 1413–1423.
Boudagher-Fadel, M.K., David Price, G., 2013. The phylogenetic and palaeogeographic evolution of the miogypsinid larger benthic foraminifera. J. Geol. Soc. 170 (1), 185–208.
Brand, U., Veizer, J., 1980. Chemical diagenesis of a multicomponent carbonate system -1: Trace elements. Journal of Sedimentary Petrology 50, 1219–1236.
Briguglio, A., Kocsis, L., Ali, F., Goeting, S., 2017. Microfacies analysis and biostratigraphic characterization of the limestone cropping out in Lumapas, Brunei Darussalam. 1st International Congress on Earth Sciences in SE Asia in Brunei Darussalam.
Bruland, K.W., Lohan, M.C., 2003. Controls of Trace Metals in Seawater. In: Holland, H. D., Turekian, K.K. (eds) Treatise on Geochemistry, vol. 6, pp 23–47.
Burke, W.H., Denison, E.R., Hetherington, A.E., Koepnick, B.R., Nelson, F.H., Otto, B.J., 1982. Variation of seawater 87Sr/86Sr throughout Phanerozoic time. Geology 10, 516–519.
Cazenave, S., Chapoulie, R., Villeneuve, G., 2003. Cathodoluminescence of synthetic and natural calcite: the effects of manganese and iron on orange emission. Mineralogy and Petrology 78 (3-4), 243–253.
Collins, J.S.H., Lee, C., Noad, J., 2003. Miocene and Pleistocene Crabs (Crustacea, Decapoda) from Sabah and Sarawak. Journal of Systematic Palaeontology 1 (3), 187–226.
Collins, D.S., Johnson, H.D., Allison, P.A., Guilpain, P., Damit, A.R., Marzo, M., 2017. Coupled 'storm-flood' depositional model: Application to the Miocene-Modern Baram Delta Province, north-west Borneo. Sedimentology 64 (5), 1203–1235.
DePaolo, D.J., Ingram, L.B., 1985. High-resolution stratigraphy with strontium isotopes. Science 227, 938–941.
Di martino, E., Taylor, P.D., Johnson, K.G., 2015. Bryozoan diversity in the Miocene of the Kutai Basin, East Kalimantan, Indonesia. Palaios 30 (1), 109–115.

Mat Fiah, N., J. Lambiase, J., 2014. Ichnology of shallow marine clastic facies in the Belait Formation, Brunei Darussalam. Bull. Geol. Soc. Malays. 60, 55–63.
Frank, M., 2002. Radiogenic isotopes. Tracers of past ocean circulation and erosional input. Reviews of Geophysics 40 (1), 1-1–1-38.
Freitas, P.S., Clarke, L.J., Kennedy, H., Richardson, C.A., Abrantes, F., 2006. Environmental and biological controls on elemental (Mg/Ca, Sr/Ca and Mn/Ca) ratios in shells of the king scallop *Pecten maximus*. Geochim. Cosmochim. Acta 70 (20), 5119–5133.
Freitas, P., Clarke, L., Kennedy, H., Richardson, C.A., 2012. The potential of combined Mg/Ca and $\delta^{18}O$ measurements within the shell of the bivalve *Pecten maximus* to estimate seawater $\delta^{18}O$ composition. Geochim. Cosmochim. Acta 70, 5119–5133.
Frijia, G., Parente, M., Di Lucia, M., Mutti, M., 2015. Carbon and Strontium isotope stratigraphy of the Upper Cretaceous (Cenomanian-Campanian) shallow-water carbonates of southern Italy: chronostratigraphic calibration of larger foraminifera biostratigraphy. Cretaceous Research 53, 110–139.
Gaillardet, J., Viers, J., Dupré, B., 2003. Trace Elements in River Waters. In: Holland, H. D., Turekian, K.K. (eds) Treatise on Geochemistry, vol. 5, pp. 225–272.
Goeting, S., Briguglio, A., Eder, W., Hohenegger, J., Roslim, A., Kocsis, L., 2018. Depth distribution of modern larger benthic foraminifera offshore Brunei Darussalam. Micropaleontology 64 (4), 299–316.
Grötsch, J., Mercadier, C., 1999. Integrated 3-D Reservoir Modeling Based on 3-D Seismic: The Tertiary Malampaya and Camago Buildups, Offshore Palawan. Philippines. AAPG Bull. 83 (11), 1703–1728.
Gradstein, F.M., Ogg, J.G., Schmitz, M.D., Ogg, G.M. 2020. A Geologic Time Scale 2020, Elsevier B.V., pp. 1390.
Haile, N.S., 1974. Borneo. Geological Society, London, Special Publications 4 (1), 333–347.
Harzhauser, M., Raven, J.G.M., Landau, B., Kocsis, L., Adnan, A., Zuschin, M., Mandic, O., Briguglio, A., 2018. Late Miocene gastropods from northern Borneo (Brunei Darussalam. Seria Formation). Palaeontographica, abt. A: Palaeozoology-Stratigraphy 313, 1–79.
Hennig-Breitfeld, J., Breitfeld, H.T., Hall, R., BouDagher-Fadel, M., Thirlwall, M., 2019. A new upper Paleogene to Neogene stratigraphy for Sarawak and Labuan in northwestern Borneo: Paleogeography of the eastern Sundaland margin. Earth-Science Reviews 190, 1–32.
Hodell, D.L., Mueller, A.P., Garrido, R.J., 1991. Variations in the strontium isotopic composition of seawater during the Neogene. Geology 19, 24–27.
Hoeksema, B.W., 2007. Delineation of the Indo-Malayan centre of maximum marine biodiversity: the Coral Triangle. In: Biogeography, Time and Place: Distributions, Barriers, and Islands, (Ed.): W. Renema. Dordrecht, The Netherlands: Springer, pp. 117–78.
Jacobsen, S.B., Kaufman, A.J., 1999. The Sr, C and O isotopic evolution of Neoproterozoic seawater. Chem. Geol. 161 (1-3), 37–57.
James, D.M.D. (Ed.), 1984. The Geology and Hydrocarbon Resources of Negara Brunei Darussalam, Bandar Seri Begawan, Muzium Brunei, 165p.
Jones, C.E., Jenkyns, H.C., Hesselbo, S.P., 1994. Strontium isotopes in Early Jurassic seawater. Geochim. Cosmochim. Acta 58 (4), 1285–1301.
Kalish, J.M., 1991. ^{13}C and ^{18}O isotopic disequilibria in fish otoliths: Metabolic and kinetic effects. Mar. Ecol. Prog. Ser. 75, 191–203.
Kessler, F.L., Jong, J., 2015. Tertiary Uplift and the Miocene Evolution of the NW Borneo Shelf Margin. Berita Sedimentologi 44, 21–57.
Kocsis, L., Briguglio, A., Roslim, A., Razak, H., Corić, S., Frijia, G., 2018. Stratigraphy and age estimate of Neogene shallow marine fossiliferous deposits in Brunei Darussalam (Ambug Hill, Tutong district). Journal of Asian Earth Sciences 158, 200–209.
Kocsis, L., Razak, H., Briguglio, A., Szabó, M., 2019. First report on a diverse Neogene fossil cartilaginous fish fauna from Borneo (Ambug Hill, Brunei Darussalam). J. Syst. Palaeontol. 17 (10), 791–819.
Kocsis, L., Usman, A., Jourdan, A.-L., Hassan, S.H., Jumat, N., Daud, D., Briguglio, A., Slik, F., Rinyu, L., Futo, I., 2020. The Bruneian record of "Borneo Amber": A regional review of fossil tree resins in the Indo-Australian Archipelago. Earth-Science Reviews 201 (103005), 1–21. https://doi.org/10.1016/j.earscirev.2019.103005.
Kocsis, L., Botfalvai, G., Qamarina, Q., Razak, H., Király, E., Lugli, F., Wings, O., Lambertz, M., Raven, H., Briguglio, A., Rabi, M., 2021. Geochemical analyses suggest stratigraphic origin and late Miocene age of reworked vertebrate remains from Penanjong Beach in Brunei Darussalam (Borneo). Historical Biology 33 (11), 2627–2638.
Koepnick, R.B., Burke, H.W., Denison, E.R., Hetherington, A.E., Nelson, F.H., Otto, J.B., Waite, E.L., 1985. Construction of the seawater $^{87}Sr/^{86}Sr$ curve for the Cenozoic and Cretaceous: supporting data. Chem. Geol. 58, 55–81.
Kusworo, A., Reich, S., Wesselingh, F.P., Santodomingo, N., G. johnson, K., Todd, J.A., Renema, W., 2015. Diversity and paleoecology of Miocene coral-associated mollusks from East Kalimantan (Indonesia). Palaios 30 (1), 116–127.
Lambiase, J.J., Cullen, B.A., 2013. Sediment supply systems of the Champion "Delta'' of NW Borneo: Implications for deep water reservoir sandstones. Journal of Asian Earth Sciences 76, 356–371.
Lambiase, J.J., Abdul Razak Damit, Simmons, M.D., Abdoerrias, R., Hussin, A., 2003. A depositional model and the stratigraphic development of modern and ancient tide-dominated deltas in NW Borneo. In: Posamentier, H.W., Hasan Sidi, F., Darman, H., Nummedal, D. (Eds.), Deltas of the Asia Pacific Region: Modern and Ancient. Society of Sedimentary Geology Special Publication 76, pp. 109–124.
Li, D., Shields-Zhou, G.A., Ling, H.F., Thirlwall, M., 2011. Dissolution methods for strontium isotope stratigraphy: Guidelines for the use of bulk carbonate and phosphorite rocks. Chem. Geol. 290 (3–4), 133–144.
Liechti, P., Roe, F.N., Haile, N.S., Kirk, H.J.C., 1960. The Geology of Sarawak, Brunei and the Western Part of North Borneo. Bulletin 3, Volumes 1&2. Geological Survey Department British Territories in Borneo. Government Printing Office, Kuching, Sarawak, pp. 360.
Lohmann, K.C., 1988. Geochemical patterns of meteoric diagenetic systems and their application to studies of paleokarst. In: James, N.P., Choquette, P.W. (Eds.), Paleokarst. Springer-Verlag, Berlin, pp. 50–80.
Lugli, F., Cipriani, A., Peretto, C., Mazzucchelli, M., Brunelli, D., 2017. In situ high spatial resolution 87Sr/86Sr ratio determination of two Middle Pleistocene (c.a. 580 ka) *Stephanorhinus hundsheimensis* teeth by LA–MC–ICP–MS. Int. J. Mass Spectrom. 412, 38–48.
Lunt, P., 2014. A review of the foraminiferal biostratigraphy of the Melinau Limestone, Sarawak. Berita Sedimentologi 29, 41–52.
Lunt, P., 2019. A new view of integrating stratigraphic and tectonic analysis in South China Sea and north Borneo basins. Journal of Asian Earth Sciences 177, 220–239.
Lunt, P., Madon, M., 2017. A review of the Sarawak Cycles: History and modern application. Bull. Geol. Soc. Malays. 63, 77–101.
McArthur, J.M., Kennedy, W.J., Chen, M., Thirlwall, M.F., Gale, A.S., 1994. Strontium isotope stratigraphy for Late Cretaceous time: Direct numerical calibration of the Sr isotope curve based on the US Western Interior. Palaeogeogr. Palaeoclimatol. Palaeoecol. 108 (1-2), 95–119.
McArthur, J.M., Howarth, R.J., Bailey, T.R., 2001. Strontium isotope stratigraphy: LOWESS version 3: Best fit to the marine Sr-isotope curve for 0–509 Ma and accompanying look-up table for deriving numerical age. Journal of Geology 109 (2), 155–170.
McArthur, J.M., Howarth, R.J., Shields, G.A., Zhou, Y., 2020. Strontium isotope stratigraphy, Chapter 7. In: Gradstein, F.M., Ogg, J.G., Schmitz, M.D., Ogg, G.M. (Eds.), A Geologic Time Scale, Elsevier B.V., Vol 1 of 2, pp. 211–238.
Mihaljevi, M., Renema, W., Welsh, K., Pandolfi, J.M., 2014. Eocene-Miocene shallow-water carbonate platforms and increased habitat diversity in Sarawak Malaysia. Palaios 29 (7), 378–391.
Morrison, K., Wong, C.L., 2003. Sequence stratigraphic framework of Northwest Borneo. Bull. Geol. Soc. Malays. 47, 127–138.
Morley, C.K., Back, S., Van Rensbergen, P., Crevello, P., Lambiase, J., 2003. Characteristics of repeated, detached, Miocene-Pliocene tectonic inversion events, in a large deltaic province on an active margin, Brunei Darussalam. Borneo. J. Struct. Geol. 25, 1147–1169.
Morley, J.R., Hasan, S.S., Morley, P.H., Jaizan Hardi M. Jais, M.H.J., Mansor, A., Aripin, M.R., Nordin, H., M., Rohaizar, H.M., 2021. Sequence biostratigraphic framework for the Oligocene to Pliocene of Malaysia: High-frequency depositional cycles driven by polar glaciation. Palaeogeogr. Palaeoclimatol. Palaeoecol.,561, 10.1016/j.palaeo.2020.110058.
Mouchi, V., Briard, J., Gaillot, S., Argant, T., Forest, V., Emmanuel, L., 2018. Reconstructing environmentsof collection site from archaeological bivalve shells: case study from oysters (Lyon, France). Journal of Archaeological Science: Reports 21, 1225–1235.
Mouchi, V., Emmanuel, L., Forest, V., Rivalan, A., 2020. Geochemistry of Bivalve Shells As Indicator ofShore Position of the 2nd Century BC. Open Quaternary 6 (4), 1–15.
Novak, V., Renema, W., 2015. Large foraminifera as environmental discriminators in Miocene mixed carbonate-siliciclastic systems. Palaios 30, 40–52.
Nuttall, C.P., 1961. Gastropoda from the Miri and Seria Formations, Tutong Road, Brunei. In: Wilford, G.E (Eds.), The Geology and Mineral Resources of Brunei and Adjacent Parts of Sarawak. Memoir 10, British Borneo Geological Survey, 73–87.
Nuttall, C.P., 1965. Report on the Haile Collection of fossil Mollusca from the Plio-Pleistocene Togopi Formation, Dent Peninsula, Sabah, Malaysia. Memoirs of the geological Survey, Borneo Region, Malaysia 16, 155–192.
Plummer, L.N., Busenberg, E., 1982. The solubilities of calcite, aragonite and vaterite in CO_2-H_2O solutions between 0 and 90 °C, and an evaluation of the aqueous model for the system $CaCO_3$-CO_2-H_2O. Geochim. Cosmochim. Acta. 46 (6), 1011–1040.
Reich, S., Warter, V., Wesselingh, F.P., Zwaan, J.C., Lourens, L., Renema, W., 2015. Paleoecological significance of stable isotope ratios in Miocene tropical shallow marine habitats (Indonesia). Palaios 30 (1), 53–65.
Renema, W., Bellwood, D.R., Braga, J.C., Bromfield, K., Hall, R., Johnson, K.G., Lunt, P., Meyer, C.P., McMonagle, L.B., Morley, R.J., O'Dea, A., Todd, J.A., Wesselingh, F.P., Wilson, M.E.J., Pandolfi, J.M., 2008. Hopping hotspots: global shifts in marine biodiversity. Science 321 (5889), 654–657.
Renema, W., Warter, V., Novak, V., Young, R.J., Marshall, N., Hasibuan, F., 2015. Ages of Miocene fossil localities in the northern Kutai basin (East Kalimantan, Indonesia). Palaios 30, 26–39.
Roslim, A., 2021. Micropalaeontological studies and palaeoenvironmental investigation of Neogene deposits, Brunei Darussalam. PhD thesis, Faculty of Science, Universiti Brunei Darussalam, pp. 239.
Roslim, A., Briguglio, A., Kocsis, L., Corić, S., Gebhardt, H., 2019. Large rotaliid foraminifera as biostratigraphic and palaeoenvironmental indicators in northwest Borneo: An example from a late Miocene section in Brunei Darussalam. Journal of Asian Earth Sciences 170, 20–28.
Roslim, A., Briguglio, A., Kocsis, L., Abd. Rahman, F., Bahrein, I. F., Goeting, S., Razak, H., 2020. Sedimentology and stratigraphy of Late Miocene outcrops (Miri and Seria formations) along Jalan Tutong in Brunei Darussalam. Bull. Geol. Soc. Malays., 70, 39–56.
Roslim, A., Briguglio, A., Kocsis, L., Goeting, S., Hofmann, Ch.–Ch., 2021. Palynology of Miocene sediments in BruneiDarussalam: first SEM investigations of pollen and spores,and their taxonomy and palaeoenvironmental interpretation. Palaeontographica Abt. B (Palaeobotany / Palaeophytology), 301 (3-6), 77–139.
Saller, A., Blake, G., 2003. Sequence stratigraphy and syndepositional tectonics of Upper Miocene and Pliocene deltaic sediments, offshore Brunei Darussalam. In: Hasan Sidi et al. (Eds) SEPM Special Publication - Tropical Deltas of Southeast Asia—Sedimentology, Stratigraphy, and Petroleum Geology. No. 76, pp. 219–234.

Sandal, S.T., 1996. The Geology and Hydrocarbon Resources of Negara Brunei Darussalam (1996 revision). Brunei Shell Petroleum Co. and Muzium Negara, Syabas Bandar Seri Begawan, Brunei Darussalam, pp. 243.

Schneider, S., Fürsich, F.T., Werner, W., 2009. Sr-isotope stratigraphy of the upper Jurassic of central Portugal (Lusitanian Basin) based on oyster shells. The International Journal of Earth Sciences 98 (8), 1949–1970.

Simon, K., Hakif, M., Barbeito, M.P.J., 2014. Sedimentology and stratigraphy of the Miocene Kampung Opak limestone (Sibuti Formation), Bekenu. Sarawak. Bull. Geol. Soc. Malays. 60, 45–53.

Sommer, S.E., 1972. Cathodoluminescence of carbonates: Characterization of cathodoluminescence from carbonate solid solutions. Chem. Geol. 9, 257–273.

Spötl, C., Vennemann, W.T., 2003. Continuous-flow IRMS analysis of carbonate minerals. Rapid Commun. Mass Spectrom. 17, 1004–1006.

Stinton, F.C., 1962. Teleostean otoliths from the upper Tertiary strata of Sarawak, Brunei, and North Borneo. British Borneo Geological Survey annual Report of 1962, 75–92.

Surge, D., Lohmann, K.C., 2008. Evaluating Mg/Ca ratios as a temperature proxy in the estuarine oyster, *Crassostrea virginica*. J. Geophys. Res. 113, G02001 https://doi.org/10.1029/2007JG000623.

Surge, D., Lohmann, K.C., Dettman, D.L., 2001. Controls on isotopic chemistry of the American oyster, *Crassostrea virginica*: implications for growth patterns. Palaeogeogr. Palaeoclimatol. Palaeoecol. 172 (3-4), 283–296.

Tate, R.B., 1974. Palaeo-environmental studies in Brunei. Brunei Museum Journal 3, 285–305.

Thorrold, S.R., Campana, S.E., Jones, C.M., Swart, P.K., 1997. Factors determining $\delta^{13}C$ and $\delta^{18}O$ fractionation in aragonitic otoliths of marine fish. Geochim. Cosmochim. Acta 61 (14), 2909–2919.

Trueman, C.N., Tuross, N., 2002. Trace Elements in Recent and Fossil Bone Apatite. Reviews in Mineralogy and Geochemistry 48 (1), 489–521.

Torres, J., Gartrell, A., Hoggmascall, N., 2011. Redefining a Sequence Stratigraphic Framework for the Miocene to Present in Brunei Darussalam: Roles of local tectonics, eustacy and sediment supply. – IPTC 15167 - International Petroleum Technology Conference, Bangkok, Thailand. pp. 12.

Ullmann, C.V., Böhm, F., Rickaby, R.E.M., Wiechert, U., Korte, C., 2013. The Giant Pacific Oyster (*Crassostrea gigas*) as a modern analog for fossil ostreoids: Isotopic (Ca, O, C) and elemental (Mg/Ca, Sr/Ca, Mn/Ca) proxies. Geochem. Geophys. Geosyst. 14, 4109–4120. https://doi.org/10.1002/ggge.20257.

Vahrenkamp, V.C., 1998. Miocene carbonates of the Luconia province, offshore Sarawak: implications for regional geology and reservoir properties from Strontium-isotope stratigraphy. Bull. Geol. Soc. Malays. 42, 1–13.

Veizer, J., 1989. Strontium isotopes in seawater through time. Annu. Rev. Earth Planet. Sci. 17 (1), 141–167.

Veizer, J., Buhl, D., Diener, A., Ebneth, S., Podlaha, O.G., Bruckschen, P., Jasper, T., Korte, C., Schaaf, M., Ala, D., Azmy, K., 1997. Strontium isotope stratigraphy: potential resolution and event correlation. Palaeogeogr. Palaeoclimatol. Palaeoecol. 132 (1-4), 65–77.

Vescogni, A., Bosellini, F.R., Cipriani, A., Gürler, G., Ilgar, A., Paganelli, E., 2014. The Dağpazarı carbonate platform (Mut Basin, Southern Turkey): Facies and environmental reconstruction of a coral reef system during the Middle Miocene Climatic Optimum. Palaeogeogr. Palaeoclimatol. Palaeoecol. 410, 213–232.

Wannier, M., Lesslar, P., Lee, C., Raven, H., Sorkhabi, R., Ibrahim, A., 2011. Geological Excursions around Miri. Ecomedia, Miri, Sarawak, Malaysia, Sarawak, p. 279.

Wierzbowski, H., Joachimski, M., 2007. Reconstruction of late Bajocian-Bathonian marine palaeoenvironments using carbon and oxygen isotope ratios of calcareous fossils from the Polish Jura Chain (central Poland). Palaeogeogr. Palaeoclimatol. Palaeoecol. 254 (3-4), 523–540.

Wilford, G.E., 1961. The geology and mineral resources of Brunei and adjacent parts of Sarawak with description of Seria and Miri Oilfields. Memoir Geological Survey Department 10, British Territories in Borneo. Brunei 10, 319.

White, W.M., 1998. The Ocean as a Chemical system. Geochemistry, an on-line textbook. Vol. 15, 645–701.

Zachos, J., Pagani, M., Sloan, L., Thomas, E., Billups, K., 2001. Trends, rhythms, and aberrations in global climate 65 Ma to present. Science 292 (5517), 686–693.

Zazzo, A., Lécuyer, C., Mariotti, A., 2004. Experimentally-controlled carbon and oxygen isotope exchange between bioapatites and water under inorganic and microbially-mediated conditions. Geochim. Cosmochim. Acta 68 (1), 1–12.